POWER QUALITY ENHANCEMENT OF AN INTER CONNECTED MESHED HYBRID MICRO GRID USING FRACTIONAL ORDER SLIDING MODE CONTROLLED UPQC

Dr. S. Jagadish Kumar[1], K. Shiva Sai [2]

[1]Associate Professor, Department of EEE, JNTUH University College Of Engineering (A) Jagtial , Kondagattu Telangana, India

[2] M. Tech Student, Department of EEE, JNTUH University College Of Engineering (A) Jagtial , Kondagattu Telangana, India

Abstract: Voltage fluctuations, harmonic distortions, and spikes are becoming more of an issue as renewable energy sources and electric car loads become more integrated into contemporary distribution networks. This research presents a networked hybrid microgrid that can control voltage and enhance power quality all at once. The UPQC in the suggested system makes use of a fractional-order sliding mode controller (FOSMC), as opposed to the proportional-integral (PI) controllers often employed in systems.. For the UPQC's shunt and series converters, the FOSMC is the standard PI controller; it precisely adjusts the voltage and current in reaction to changing loads and situations including renewable energy generation. Coordination of the UPQC with the battery energy storage system is an integral part of the integrated modelling and control approach for the hybrid AC-DC microgrid. By improving the entire interconnected hybrid microgrid power quality and reliability, the simulation results show that the proposed FOSMC-based UPQC is more effective than the traditional PI-controlled UPQC at mitigating power quality problems.

Key terms - Power quality, Harmonic distortion, Fractional-order sliding mode controller, and Battery energy storage systems.

I.INTRODUCTION: Traditional alternating current (AC) microgrids have a lot of trouble integrating DG units, EVs, and BESSs due to the many power conversion steps needed to enable dependable communication [2],[3],[4]. Cascaded DC-DC and DC-AC converters are the most typical means of connecting photovoltaic (PV) DGs and BESSs to the AC grid [4],[8]. In addition, further conversion stages are required for many contemporary loads, including as electric car chargers, office equipment, and household appliances, which run on low-voltage DC (LVDC) when supplied by AC systems [3] [6] . The system's complexity and overall efficiency are both increased by these many conversion steps [2],[6]. Voltage fluctuations, imbalances, harmonics, and spikes are examples of power quality (PQ) concerns caused by the systems' heavy reliance on power electronic converters [1],[13],[16]. Concerns about voltage spikes may arise from the reversal of power flow that results from widespread usage of renewable energy sources (RES)[1],[15]. Because of voltage limitation breaches and thermal saturation of network components, classical AC microgrids have a limited capacity [5],[6], for hosting. Due to these difficulties, a more sophisticated grid design that can handle both static and dynamic loads is critically required. New hybrid AC-DC microgrids provide a possible way around these restrictions [6],[8]. These microgrids are designed to be more flexible by integrating AC and DC sub grids. Through the use of interlinking converters and several power flow pathways, meshed hybrid microgrid systems also provide enhanced operational dependability and flexibility[9],[10],[17]

To reduce the impact of power quality problems, the Unified Power Quality Conditioner (UPQC) is crucial, since it combines the functions of a distribution static compensator (D-STATCOM) and a dynamic voltage restorer (DVR) [12], [14]. It

ISSN: 3049-0952
www.jsetms.com

maintains a steady voltage at the PCC and checks for harmonics in the current and reactive power. When faced with nonlinear, unpredictable, and dynamic operating situations, traditional UPQC systems and their PI controllers prove to be inadequate [14], [15]. A Fractional-Order Sliding Mode Controller (FOSMC) is suggested as a solution to these problems in order to regulate the UPQC's series and shunt converters in a connected hybrid microgrid [20], [21], [22]. In comparison to traditional PI-based controllers, the FOSMC has better dynamic responsiveness, parameter change resilience, and disturbance rejection capabilities [21], [22], [23]. The proposed system uses a mesh hybrid AC-DC microgrid design to include PV generation, EV loads, and BESS [2], [8], [9]. Because of this, power management coordination and enhanced PQ performance are both achievable [8], [9]. As opposed to PV-based PQ improvement approaches, the suggested UPQC with BESS guarantees continuous bidirectional power flow and precludes active power limitation during reactive power support [8], [18]. The constraints of intermittent generation are therefore removed. The effective energy buffering made possible by BESS's DC link connection enhances system stability in the face of changes to RES and grid shocks [18], [24]. Many benefits are available from the proposed interconnected hybrid microgrid that uses UPQC based on FOSMC: It achieves near-unity power factor operation by balancing and preventing distortion where the reactive and harmonic components of the load currents are corrected at the LVAC point of common coupling (PCC) [13], [14]. The FOSMC allows for accurate voltage control under different circumstances of PV generation and EV loads, achieving superior dynamic performance and resilience [21], [23]. The system continues to operate reliably even when faced with disturbances such as voltage sag, swell, unbalanced loads, or converter failures [14], [23]. Furthermore, dispersed energy resources can be better utilized, electricity can flow in both directions, and power sharing can be optimized through the coordinated integration of PV, EV, and BESS [8], [9], [18]. Compared with traditional AC microgrids, the meshed hybrid design enhances system hosting capacity, flexibility, and overall dependability [2], [6], [9], [10].

II. PROPOSED SYSTEM

The Figure 1(a), we can see a UPQC example of an LV_{ac} microgrid system. The BESS is connected to the UPQC dc connector via a dc-dc converter in this arrangement. An LV_{ac} grid incorporates a large number of photovoltaic (PV) DG sources, and a network of LV_{dc} buses connects charging stations for electric vehicles. Figure 1(b) depicts one possible design for the linked hybrid microgrid. The vline is accompanied with an improved UPQC dc connection. As can be seen in Figure 1(a), the BESS connection has not altered. Connecting PV-based DGs to the LV_{dc} line is accomplished via the use of dc-dc converters. Electric vehicles and dc loads may be connected anywhere using a dc-dc converter. The first stage in wiring electric vehicles and solar power systems is to connect the dc-ac converters to the ac and dc distribution lines. Because dc-ac converters are so widely available, it is feasible to construct several linked distribution loops. The BESS maintains a steady dc connection voltage in the event of UPQC power outages. Through active power exchange with the LV_{dc} grid, the BESS maintains a steady dc connection voltage. Furthermore, the LV_{dc} line losses required for operation are supplied by the BESS. Active power exchange between the LV_{ac} and LV_{dc} grids is made possible by the two parallel grids in the proposed mesh hybrid network. The UPQC controls reactive power, allowing active power to flow in either way across a network of connected hybrid microgrids. The UPQC ensures the usage of DG dc-ac converters for active power exchange and reactive power support. The DG converter may transfer active power between the LV_{ac} and LV_{dc} grids using grid code constraints to maintain the voltage at the end of the LV_{ac} bus within acceptable limits. Power plants and electric vehicles connected to the LV_{dc} grid will keep running regardless of the fate of DG converters. The UPQC is heavily used in this research. No matter how bad the power loss is, this maintains the LV_{ac} PCC load voltage within the limits set by the grid code. It keeps the grid currents balanced, sinusoidal, and with a unity power factor, and it also provides the reactive and harmonic components of the load current. By using the energy stored in the dc link of UPQC, the LV_{ac} grid may be used in place of active power as needed. And UPQC in a mesh-hybrid microgrid lets the LV_{ac} and LV_{dc} grids communicate via several transfer channels. A UPQC regulates the active power flow between the LV_{ac} and LV_{dc} grids in the case of excessive PV production, severe EV demand, or DG converter failure. Since the UPQC takes care of the reactive power requirements of the LV_{ac} loads, the DG converters connected to the LV_{ac} and LV_{dc} buses may not need reactive power at all. The efficiency of the converters is enhanced as a result.

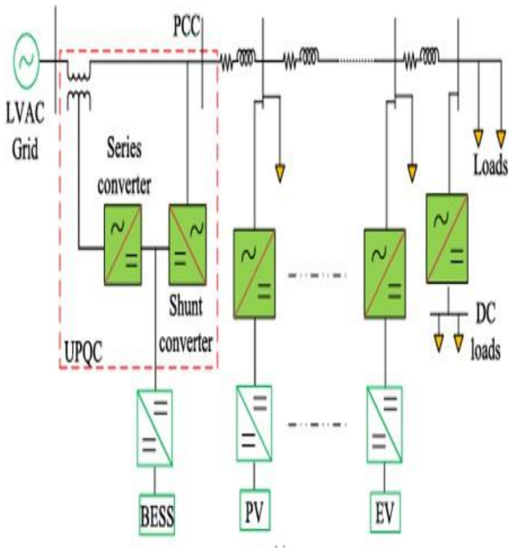

(a)

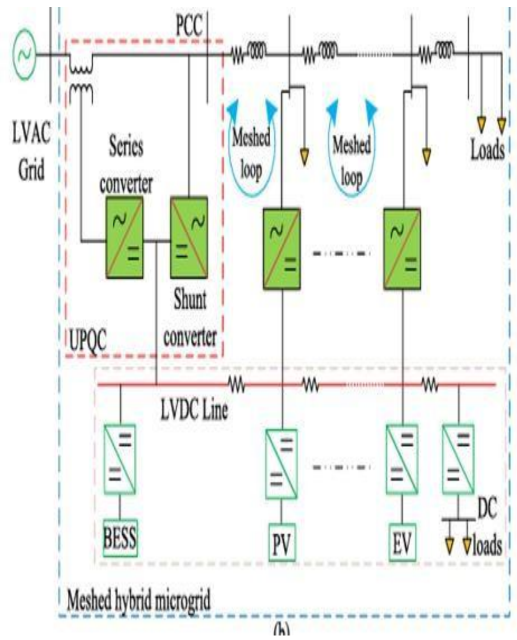

(b)

Fig.1. System configuration. (a) UPQC connected conventional ac micro grid . (b) Proposed UPQC enabled meshed hybrid microgrid.

A traditional UPQC-based LV_{ac} microgrid may have its operating capacity significantly enhanced by connecting it to a parallel low-voltage dc (LV_{dc}) distribution line, as shown in Figure 5.1(b). This LVdc line is established by extending the UPQC's dc connection throughout the distribution network in conjunction with the current LV_{ac} feeder. It is possible to directly integrate dc-based energy sources and loads into this system thanks to the UPQC dc link, which acts as a backbone dc bus. Following industry norms, the BESS is hardwired into the UPQC dc link, which guarantees constant power storage support and voltage control on the dc-link. However, the dc connection now plays an integral role in the power exchange across the whole system, rather of only acting as a localised energy buffer as in the previous system. First, dc-dc converters physically link the PV-based DG units to the line. Efficiency is improved and converter stress LV_{dc} is reduced with direct dc integration by eliminating unnecessary dc-ac-dc conversion steps. When LV_{dc} lines are connected to dc loads, such as electric vehicle charging stations, dc-dc converters enable the flexible management of voltage and control of power. Updating the dc-ac converters connected to PV and EV systems is a crucial aspect of connecting the LV_{ac} and LV_{dc} distribution lines. These converters enable bidirectional power transmission between the hybrid microgrid's alternating current and direct current subsystems by establishing many linked loops. The meshed topology's redundant power lines increase system reliability and resilience against component failures.

III. PROPOSED POWER MANAGEMENT ALGORITHM

The objectives of our power management algorithm are as follows (1) maintaining a power factor of one for balanced and sinusoidal grid currents;(2) actively routeing power between the LV_{ac} and LV_{dc} lines during peak load or generation scenarios; (3) maintaining a nominal voltage magnitude for the LV_{ac} PCC; and (4) controlling the active power exchange between the LV_{ac} and LV_{dc} lines in the event of a dc-ac converter failure. The UPQC series converter prevents voltage fluctuations in the LV_{ac} PCC from affecting the grid voltage. Additionally, with the assistance of UPQC, a shunt converter, LV_{ac} loads may use the grid's balanced and sinusoidal current at unity power factor. It is possible for this converter to generate reactive load current, imbalanced current, and harmonics. It is also possible to implement active power switching using dc-ac converters connected to LV_{ac} and LV_{dc} grids. The suggested method for managing electricity is shown in Figure 2 by a flow diagram. Both normal operation and converter fault operation are shown in Figure 1(b). Normal operation happens when every dc-ac converter is functioning correctly, whereas converter fault operation happens when some of the converters are faulty. You may find the active power references for the UPQC shunt converter and PV/EV dc-ac converters for each working mode. P_{net}, which stands for active power of the net load on the LVdc line, may be determined in the following way:

$P_{net} = I = 1 \sum n \, (P_{EV-i} + P_{dc\,L-I} - P_{PV-i})$ (1).

A) Regular Function

Under these conditions, all of the dc-ac converters are functioning as planned, and everything is running well. Electric car and solar system dc-ac converters have the following total power rating (St−rat):

$S_{t\text{-}rat} = I = 1 \sum n \, (S_{r\,EV-i} + S_{r\,PV-i})$ (2)

The electric vehicle (EV) rating is denoted by $s_{r\,E\,V-i}$, whereas the photovoltaic (PV) dc—ac converter rating is represented by $S_{r\,P\,V-i}$. Power plants and electric vehicles actively contribute to power grids by means of their dc-ac converters, which use the P_{net} value from (1). Because UPQC meets the reactive power requirements of LV_{ac} loads, the grid current is balanced and sinusoidal at unity power factor. This is why the reactive power reference of the PV/EV dc-ac converters is set to zero in the proposed technique. However, reactive power may be handled by this converter if necessary. A drop in the converter's active power is an undesirable side effect. When P_{net} is positive for DC grids, it means that total power demand is higher than generating capacity. A negative v occurs in a DC grid when the producing capacity, as measured by sources such as solar PV and EVs, is less than the demand for power. The production and consumption of DC grid electricity are in equilibrium when P_{net} t= 0. Assuming the derivative of St−rat from equation (2) is larger than or equal to the absolute value of P_{net}, the active power for the ith dc—ac converter of PV and EV is:

$P_{PV-i}* = P_{net} \times S_{r\,PV-i} \,/\, S_{t\text{-}rat}$

$P_{EV-i}* = P_{net} \times S_{r\,EV-I} \,/\, S_{t\text{-}rat}$ (3)

The PV system's active power reference is denoted by P^*_{PV-i}, whereas the EV $_{dc—ac}$ converters' active power reference is denoted by P_{EV-i}. If $S_{t-rat} < | P_{net}\, t|$, the ith dc—ac converter of PV and EV will exchange the maximum active power from the grid, and they are supplied in the following way: $P^*_{EV-i} = S_{rEV-i}$

$P^*_{EV-I} = S_{r\,EV-i}$ (4)

To meet the additional power needs of the LVdc line, the UPQC shunt converter trades in the grid's active power balance. So, the active power reference for the UPQC shunt converter is the equation.

$P_{D^*} = P_{net} - S_{t\text{-}rat}$ (5)

In this configuration, when the LVdc line is under severe loading, power is transferred from an LV_{ac} source to it via a UPQC shunt converter. Therefore, the LVac line voltage profile is superior for both peak demand and generation.

B) Operating a Converter Fault

A defective PV/EV dc—ac converter is the source of electricity for the connected hybrid microgrid in this instance. The next step is to employ healthy PV/EV dc—ac converters to split the active electricity flowing between the alternating current and direct current network systems. Hence, the active power of the ith PV/EV converter is defined as

$P_{C-i}* = S_{t\text{-}rat} - S_{r-m}\, P_{net} \times S_{rC-I} \,/\, S_{t\text{-}rat} - S_{r-m}$

if $| P_{net} | \leq S_{t\text{-}rat} - S_{r-m}$ (6)

Active power of the PV/EV dc-ac converter is denoted by $P_{C\backslash i}$. The sign S_{rC-i} represents the apparent power rating of the PV/EV dc-ac converter, whereas the symbol Sr−m represents the faulty unit.

$P_{D}* = P_{net} - (S_{t\text{-}rat} - S_{r-m})$ (7)

conversion of direct current to alternating current for vehicles and photovoltaic systems on the mth bus. Eliminating the defective PV/EV converters puts a halt to the operation. Based on its power rating, each of the operational The active power is shared by PV/EV dc-ac converters. To calculate the active power reference for the UPQC shunt converter, utilise Equations (1) and (2) together with Sr−m, if the total power rating of the healthy dc-ac converter is less than | P_{net} |.Therefore, the suggested UPQC hybrid microgrid architecture ensures that active power exchange continues even after the defective dc-ac converter is removed. The traditional design of microgrids also precludes this option, as seen in Figure 1(a). The suggested setup uses a single PV/EV dc—ac converter for both power generation and electrical load.

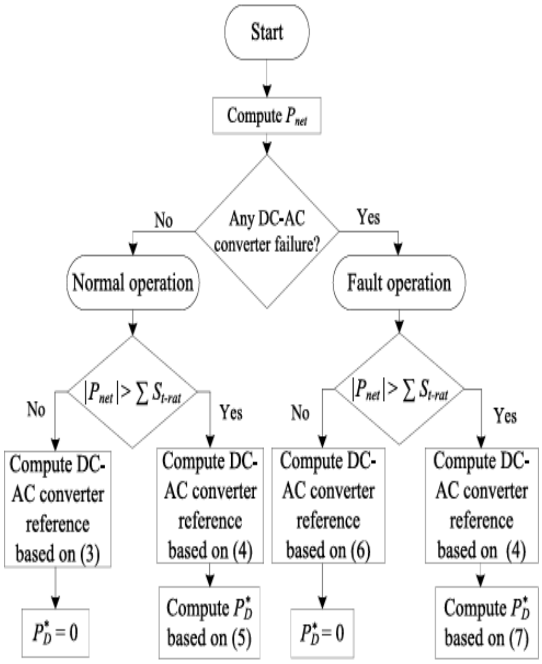

Fig.2. Flowchart for power management.

IV CONTROL OF POWER CONVERTERS

The meshed hybrid microgrid is set up using several power converters. The suggested configuration's control diagram is seen in Figure .3 This section provides a description of UPQC converters, BESS dc-dc converters, photovoltaics, and electric vehicle dc—ac converters.

A) UPQC Converters

A multitude of nonlinear loads may be supported by the LVac grid. The control algorithm calculates the harmonic, reactive, and unbalance currents; the UPQC shunt converter provides the LVac load current components. Furthermore, harmonics and fluctuations in the supply voltage are mitigated by UPQC's series converter. Here we will go over the UPQC shunt and series converters' control strategy.

B) UPQC Shunt Converter:

Supplying reactive and harmonic power to the LV_{ac} load is the principal control function of the UPQC shunt converter. This converter also enables active power exchange, which is an extra need. This converter will respond to changes in the electrical current at all times. By using an ISCT, it is feasible to integrate supplies from both the LV_{ac} and LV_{dc} grids. The reference currents i^*_{daa}, i^*_{dab}, and i^*_{dac} are used by the UPQC shunt converter for the purpose of active power distribution.

$$i^*_{dab} = \frac{v^+_{lb1}}{(v^+_{la1})^2 + (v^+_{lb1})^2 + (v^+_{lc1})^2} P^*_D$$
$$i^*_{dac} = \frac{v^+_{lc1}}{(v^+_{la1})^2 + (v^+_{lb1})^2 + (v^+_{lc1})^2} P^*_D \quad (8)$$

The three-phase positive sequence voltage at LV_{ac} PCC is $v^+_{la1} v^+_{lb1}$, and v^+_{lc1}, and the UPQC shunt converter uses P* D as its dc power reference. In normal operations, P*D is obtained from equation (5.5), but in fault operations, it is obtained from equation (5.7). The UPQC shunt converter use the reference currents (i^*_{dha}, i^*_{dhb}, and i^*_{dhc}) to distribute the reactive and harmonic components of the LV_{ac} load currents.

$$i^*_{dha} = i_{lva} - (v^+_{la1} \,/\, (v^+_{la1})^2 + (v^+_{lb1})^2 + (v^+_{lc1}) * P_{lv}$$

$$i^*_{dhb} = i_{lvb} - \frac{v^+_{lb1}}{(v^+_{la1})^2 + (v^+_{lb1})^2 + (v^+_{lc1})^2} P_{lv}$$
$$i^*_{dhc} = i_{lvc} - \frac{v^+_{lc1}}{(v^+_{la1})^2 + (v^+_{lb1})^2 + (v^+_{lc1})^2} P_{lv}$$

(9)

P_{lv} is the average load power measured at PCC, while i_{lva}, i_{lvb}, and i_{lvc} are the instantaneous LV_{ac} load currents recorded at PCC. According to equations (5.8) and (5.9), the UPQC shunt converter's reference currents are as follows: i^*_{sha}, i^*_{shb}, and i^*_{shc}.

$$i_{sha}* = i_{lva} - (v^+_{la1})^2 /(v^+_{la1})^2 + (v^+_{lb1})^2 + (v^+_{lc1})^2 * (P_{lv} - P_D*)$$

$$i^*_{shb} = i_{lvb} - \frac{v^+_{lb1}}{(v^+_{la1})^2 + (v^+_{lb1})^2 + (v^+_{lc1})^2}(P_{lv} - P^*_D)$$

$$i^*_{shc} = i_{lvc} - \frac{v^+_{lc1}}{(v^+_{la1})^2 + (v^+_{lb1})^2 + (v^+_{lc1})^2}(P_{lv} - P^*_D) \quad (10)$$

A hysteresis-based current controller is one possible method of controlling the UPQC shunt converter [22]. By comparing the actual currents of the UPQC shunt converter with reference currents obtained from the same device, the controller is able to compute the pulses (10).

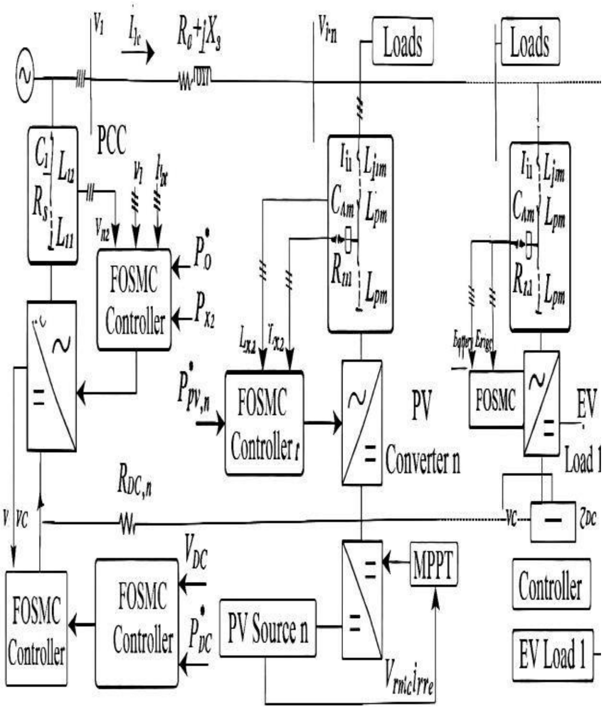

Fig.3 Overall control diagram of the meshed hybrid microgrid

C) UPQC Series Converter:

The series converter controls the PCC voltage such that it stays balanced and sinusoidal at its nominal value, regardless of grid voltage instability like sag/swell, imbalance, or harmonics. Regardless of changes in the grid voltage, this converter maintains a constant PCC voltage by the exchange of active power from the dc link [23]. When the grid voltage is low, active power is sent to the dc-link via the series converter, and when the voltage is high, it goes to the other way around. In order to maintain the dc-link voltage at its reference value, the BESS actively controls the power exchange. It is necessary to provide the series converter with accurate reference three-phase voltages in order to maintain a constant PCC voltage even in the event of a grid outage.

The voltage reference for a series converter is the low-voltage AC (LV_{ac}) terminal voltage at the grid, namely the harmonic and fundamental positive-sequence components. This dissection may be able to correct voltage irregularities including sag, swell, and harmonics. A consequence of adding the voltages in the harmonic and fundamental positive-sequence components is the total voltage at the grid terminals,

$$V_t = v_{t1} + v_{trest} \quad (11)$$

The basic positive sequence component is denoted by v_{t1} in the LV_{ac} grid terminal voltage, whereas the harmonic voltage component is represented by v_{trest}. V_{f1} is the series converter voltage's first positive sequence component. At PCC, the UPQC series converter is responsible for balancing the three phases of the voltage. Here is one approach to represent the reference voltage (V_l*) at PCC using Kirchhoff's voltage law (KVL):

$$V_I * = V_{t1} + V_{f1} \quad (12)$$

The fundamental positive sequence component of the LV_{ac} grid terminal voltage is vt1, the harmonic voltage component is vtrest, and the initial positive sequence component of the series converter voltage is V f1. At PCC, the UPQC series converter is responsible for balancing the three phases of the voltage. Here is one approach to represent the reference voltage (V_l*) at PCC using Kirchhoff's voltage law (KVL):

$$V_{f1} = v_1^* - V_{T1}$$

$$V_{f1}\angle\phi_{f1} = V_I\angle 0 - V_{t1}\angle\delta_{t1} \quad (13)$$

This is the answer to the fifth equation, where V_{f1} is the voltage magnitude and φf 1 is the phase angle.

$$V_{f1} = \pm V_{t1} \text{ square root of } K^2 + 1 - 2K\cos\delta_{t1} \quad (14)$$

$$\phi_{f1} = \tan{-1} (\sin Q_{t1} / \cos Q - k) \quad (15)$$

V_l/V_{t1} is abbreviated as K. Voltage sag is indicated by a positive value of V_{f1}, whilst voltage swell is shown by a negative value. The phase of the basic positive voltage series at the grid terminals is represented by the angle δt1.To further mitigate the effects of harmonics in the grid terminal voltage, the series converter further supplies the harmonic voltage component. The voltage v*f, which is shown below, is injected by the UPQC series converter.

$$V^*_f = v_{f1} - v_{lrest} \quad (16)$$

the source terminal voltage's harmonic component is represented by v_{trest}. The injected voltage of the UPQC series converter, which is enabled by (14)-(16):

$$v_{fa}^* = \sqrt{2}\, V_{f1} \sin(\omega t+\phi_{f1}) - v_{tarest}$$

$$v_{fb}^* = \sqrt{2}\, V_{f1} \sin(\omega t+ \phi_{f1} - 2\pi/3) - v_{tbrest}$$

$$v_{fc}^* = \sqrt{2} V_{f1} \sin(\omega t+ \phi_{f1} - 4\pi/3) - v_{tcrest} \quad (17)$$

The PCC voltage is maintained at its nominal value by injecting these voltages by means of the UPQC series converter. It is possible to control the UPQC series converter using a voltage controller that is based on hysteresis. This controller determines when to generate pulses for the UPQC series converter by comparing the converter's actual voltages to a reference value (17).

D) BESS DC–DC Converter

The UPQC converters' dc connection is connected to the BESS's dc-dc converter. It enables active power exchange and supplies DC grid power losses in the case of an LV_{ac} voltage disturbance. The BESS dc-dc converter is primarily responsible for controlling the voltage on the UPQC dc-link. The dc link receives active power from the BESS dc-dc converter, which is injected into the LV_{ac} grid via the UPQC to maintain an appropriate voltage level even when the grid voltage drops. On the other hand, the UPQC stores the additional active power it utilises to regulate the BESS's PCC voltage in the event of a voltage spike. Whether the BESS is consuming or generating power dictates the direction of current in the dc-dc converter; this maintains a consistent dc-link voltage in the UPQC. The control method looks at the difference between the reference value (V_{dc}) and the observed dc-link voltage (V_{dc}) to find the voltage error. A proportional-integral (PI) controller looks at this error signal to make sure the BESS dc-dc converter gets the right switching pulses [24].

V. PROPOSED FOSMC CONTROLLER

Combining the adaptability of fractional-order calculus with the robustness of SMC, the Fractional-Order Sliding Mode Controller (FOSMC) is a complex nonlinear control system. When compared to conventional integer-order controllers, FOSMC employs additional tuning parameters, such as fractional derivatives and integrals, to enhance system performance in unpredictable and disruptive conditions. To direct system states along predetermined trajectories, traditional SMC makes use of a sliding surface. Although it is flexible, conventional SMC isn't chatter-proof. To get around these problems, FOSMC uses a fractional-order sliding surface outline to make it more dynamically responsive and less oscillatory.One way to represent the generalised sliding surface is using the formula:

$$S(t) = D_{\alpha e}(t) + \lambda_e(t) \quad (18)$$

- e(t) = error signal (reference − actual),
- Dα = fractional derivative operator (0<α<1),
- λ= positive control gain.

An analogous control plus a switching control component make up the FOSMC control law:

$$u(t) = u_{eq}(t) + u_{sw}(t) \quad (19)$$

Usually, the switching control is described as:

$$u_{sw}(t) = -K \cdot \sin(S(t)) \quad (20)$$

here the switching gain is denoted by K. Saturation or smooth approximations are often used in lieu of the sign function to decrease chattering.

VI. SIMULATION RESULTS

An interconnected hybrid microgrid with two buses and UPQC is used in this field of research. Bus 2 is where the PV supply is connected, whereas bus 1 is where the EV load is located. Furthermore, dc loads are assessed using the LV_{dc} line, whereas ac loads are done using the LV_{ac} line.

TABLE 1 SIMULATION PARAMETERS

System quantities	Values
LVac grid voltage	400 v
LVdc grid voltage	1.2 KV
UPQC series converter	Transformer ratio =1 :1, S_{rse} = 50kVA, (L_f) = 3 mH (C_f) = 20 µF (R_d) = 40 Ω
UPQC shunt converter	(S_{rsh}) = 50 kVA (L_{s1}) = 2 mH C_s) = 20 µF (R_s) = 40 Ω (L_{s2}) = 1 mH
PV dc-ac converter	(S_{rPV}) = 50 kVA (C_{dc1}) = 2200 µF (L_{fm1}) = 6 mH (L'_{fm1}) = 68 µH (C_{fm1}) = 10 µF (R_{d1}) = 1 Ω
EV dc-ac converter	(S_{rEV}) = 25 kVA (C_{dc2}) = 2200 µF (L_{fm2}) = 4 mH (L'_{fm2}) = 45 µH (L'_{fm2}) = 45 µH (C_{fm2}) = 15 µF (R_{d2}) = 1 Ω

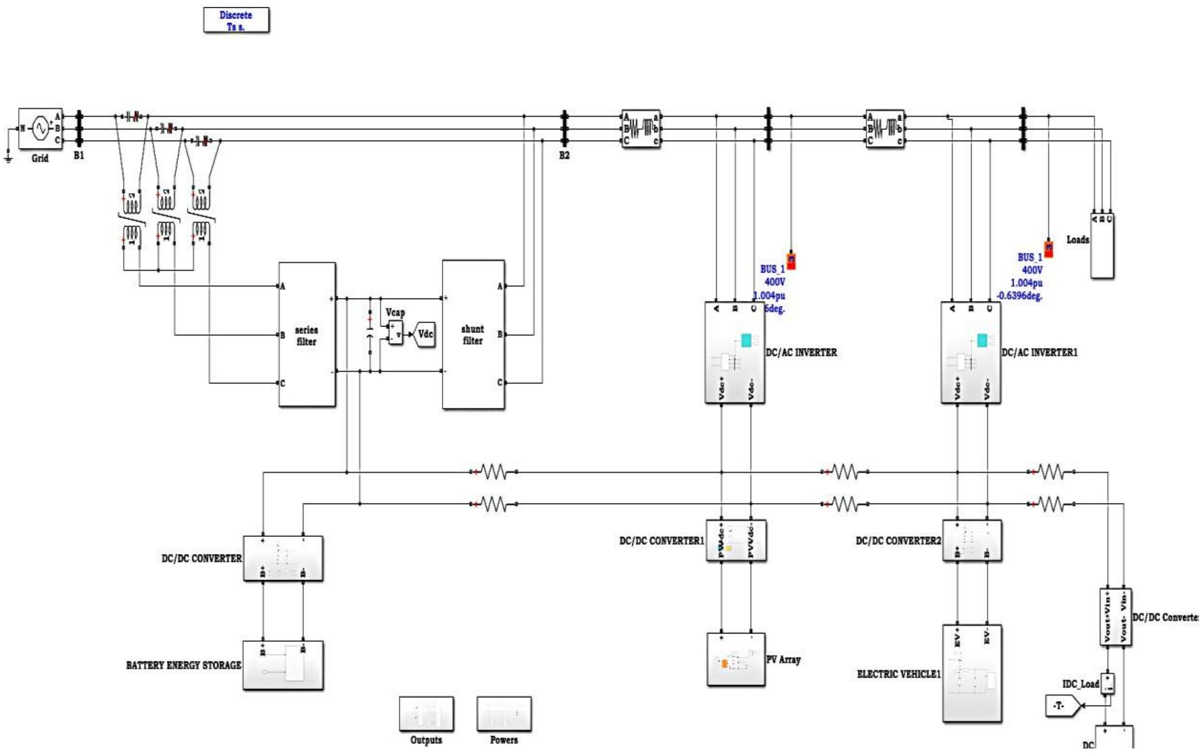

Fig.4. An UPQC-enabled mesh hybrid microgrid's MATLAB/SIMULINK circuit

A) (PI CONTROLLER)

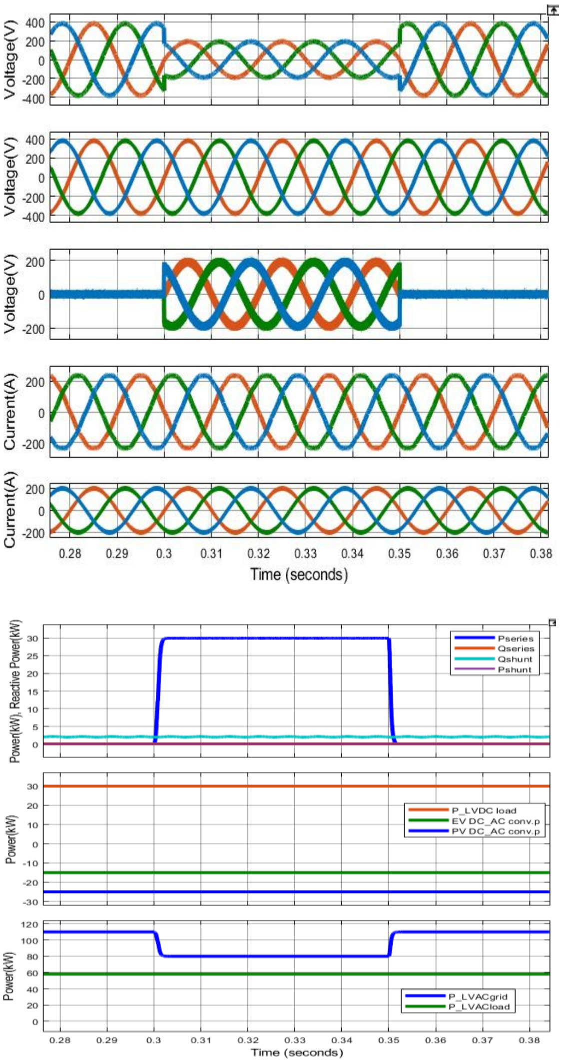

Fig.5 Results of the grid voltage sag operation simulation. (a) Voltages on the grid. (a) The voltage at the converter for converting electricity. C, the UPQC series converter voltage. d) The currents flowing through the LV_{ac} load at the PCC. e. Grid currents. (f) Powers UPQC series and shunt transistors. (h) LV_{dc} load, which includes the powers

of the dc-ac converter. the powers of the LVac grid and the load.

The graphs shows the grid voltage sag operation where voltage sag shows in the period from 0.30 to 0.35. and the upqc series converter is injected the voltage to reduce the voltage sag and the fluctuations and spikes present while using pi controller.

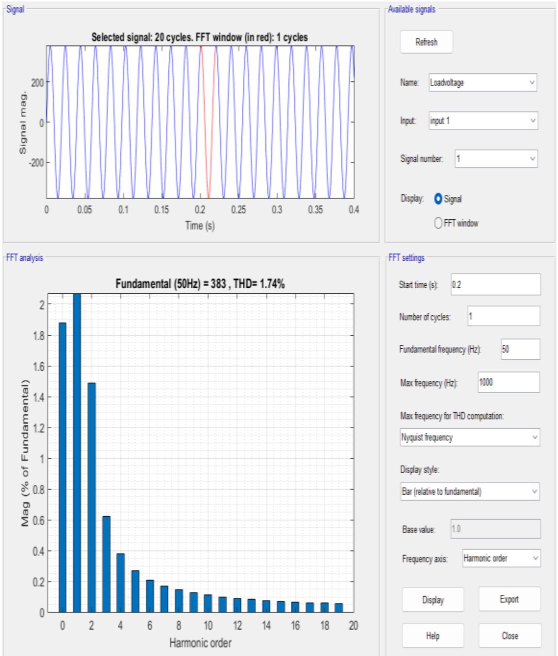

Fig 6 Voltage at load THD%

The above figure shows the FFT analysis of load voltage is 2.64 percentage while pi controller.

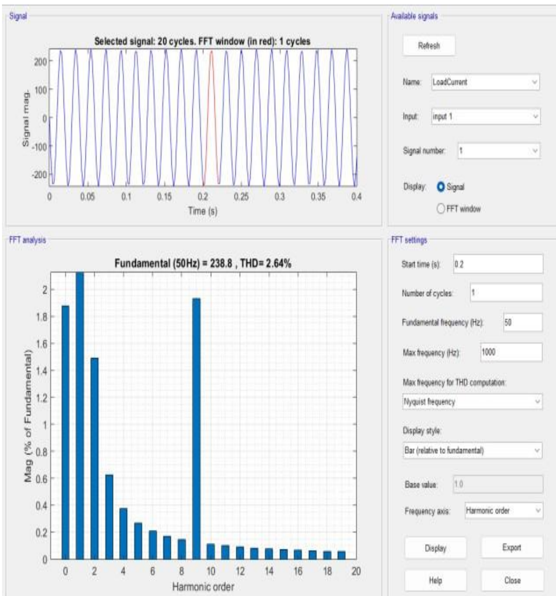

Fig.7 Load current THD%

The above figure shows the FFT analysis of load current shows the 1.74 percentage, while using pi controller.

ISSN: 3049-0952
www.jsetms.com

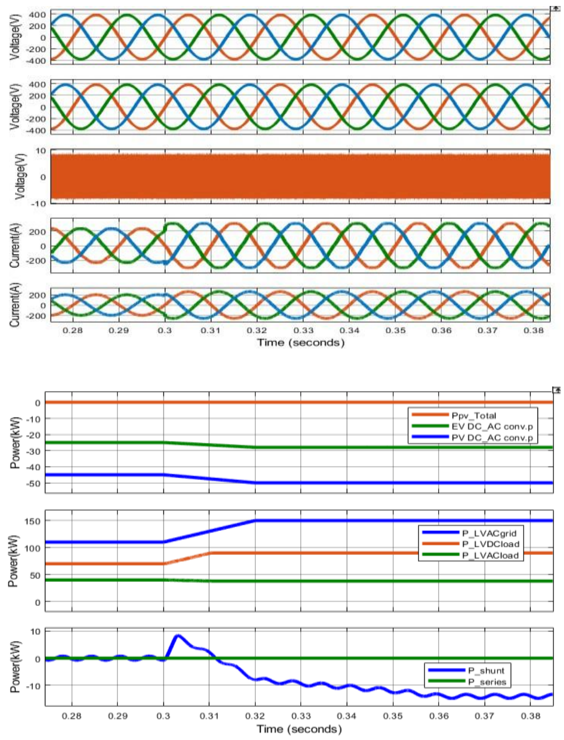

Fig.8 Simulation results for high dc load operation.(a) Grid voltages.(b)Voltage at PCC. (c) UPQC series converter voltages. (d) LV_{ac} load currents at PCC. (e) Grid currents.(f) PV generation, EV, and PV dc—ac converter powers.(g) Grid,LV_{ac} ,and LV_{dc} powers. (h) UPQC shunt and series converter powers.

The above simulation results shows when the high loads are on the dc supply.And when the load increases suddenly the converter powers and ev powers and pv power and changes suddenly and the spikes visible in the above diagram.

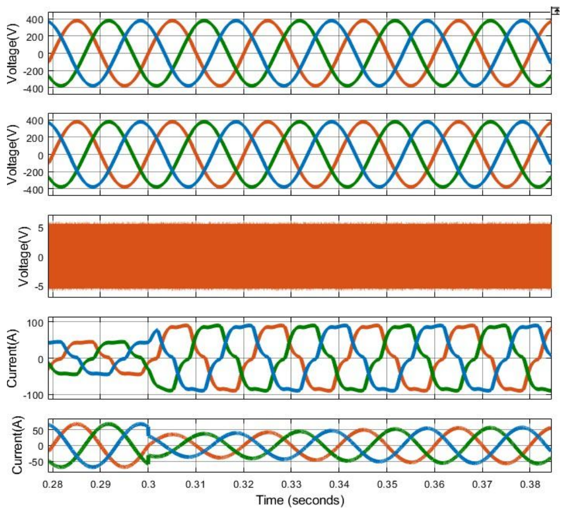

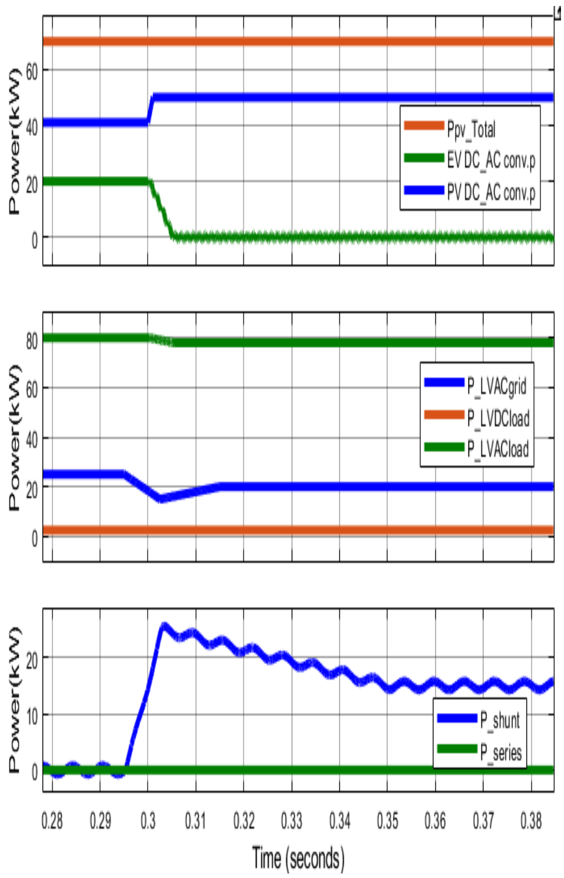

Fig.9: Electric vehicle dc-ac converter breakdown operation simulation findings. (a) Voltages on the grid. (a) Voltages measured at the PCC. The voltage of the UPQC series converter (c). d) Currents across the LV_{ac} load at the PCC. e. Currents in the grid. (f) The powers of photovoltaic (PV) generating, electric vehicles (EVs), and PV dc—ac converters. g) Powers generated by the Grid, LV_{ac}, and LV_{dc}. (h) Power from the UPQC shunt and the series converter.

The above graphs shows the converter failure operation , The three-phase voltages remain balanced, and the converter injects the required voltage during the disturbance period. The source current becomes distorted during the transition, while the load current remains balanced and sinusoidal. The PV system continues to generate nearly constant power throughout the operation. After the disturbance, the converter transfers more power to the DC side, while the AC load power remains almost constant. The shunt converter power increases during compensation and then gradually settles to a steady value, ensuring stable system operation.

B) (FOSMC CONTROLLER)

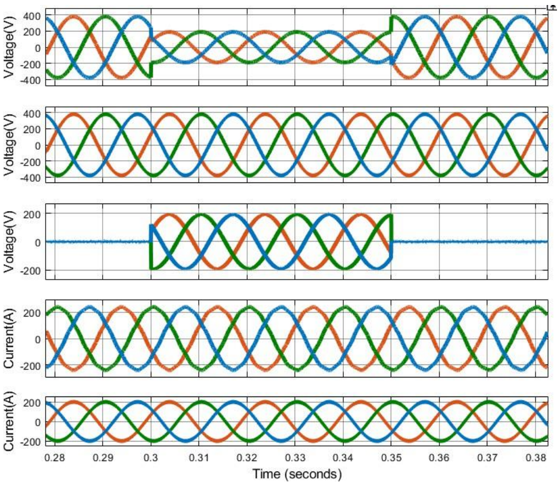

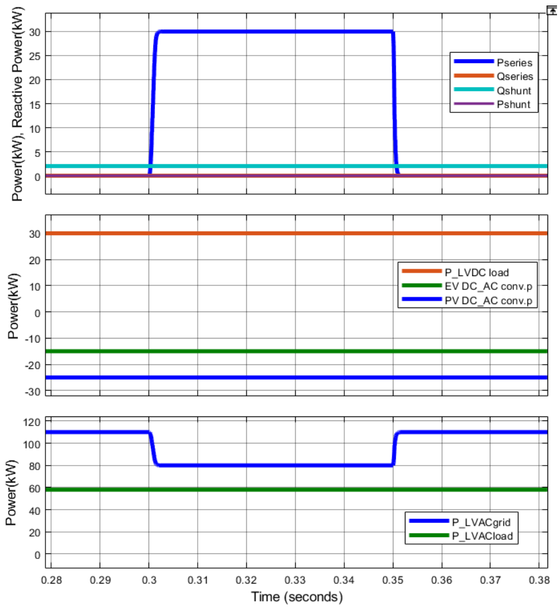

Fig. 10 (A) shows how the grid voltage sag simulation operation performed. a) Voltages on the grid. (a) The voltage of the power converter. The converter voltage of the UPQC series is C. d. Grid currents; e. Currents propagating via the LV_{ac} load at the PCC. the shunt and UPQC series transistors are powered. g) Power supply for dc-ac converters and LV_{dc} loads. workload and voltage on the low-voltage grid.

The above simulation results shows the grid voltage sag operation the simulation the after 0.30 to 0.35 the voltage sag is observed. And series converter is injected the voltage to for system optimization. The spikes and fluctuation eliminated, while using FOSMC controller.

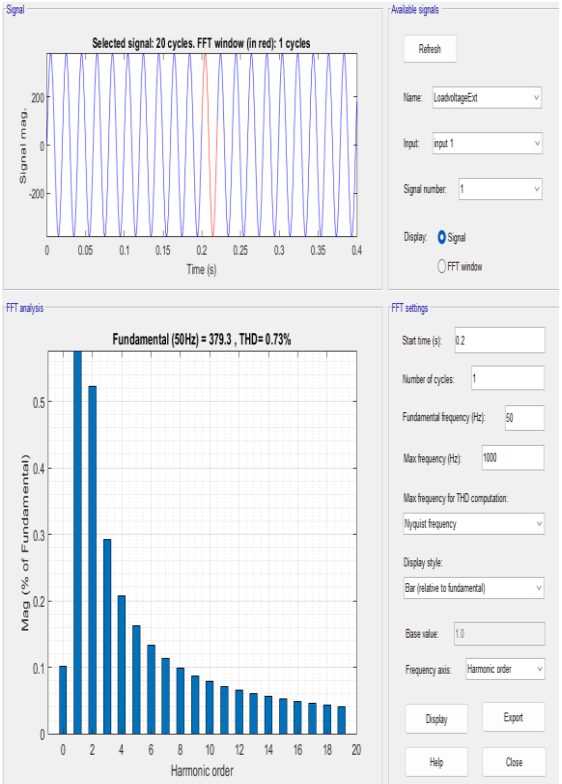

Fig.11 Current at load THD%

The above figure shows the total harmonic distortion of the load current is 0.73 percentage after replacing the PI controller to FOSMC controller, the THD performance is increased.

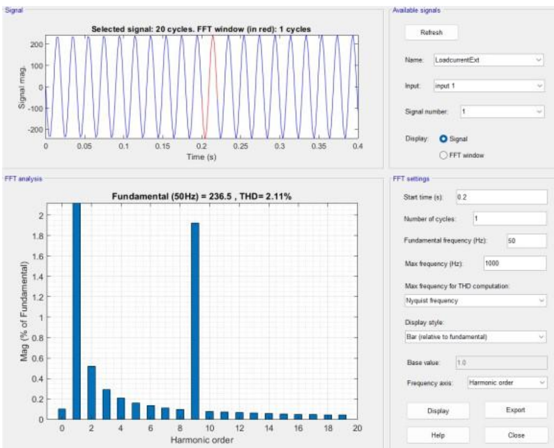

Fig.12 Total harmonic distortion (THD) percentage loads at voltage

The figure shows the total THD analysis , shows 2.11 percentage, the total harmonic distortion is improved.

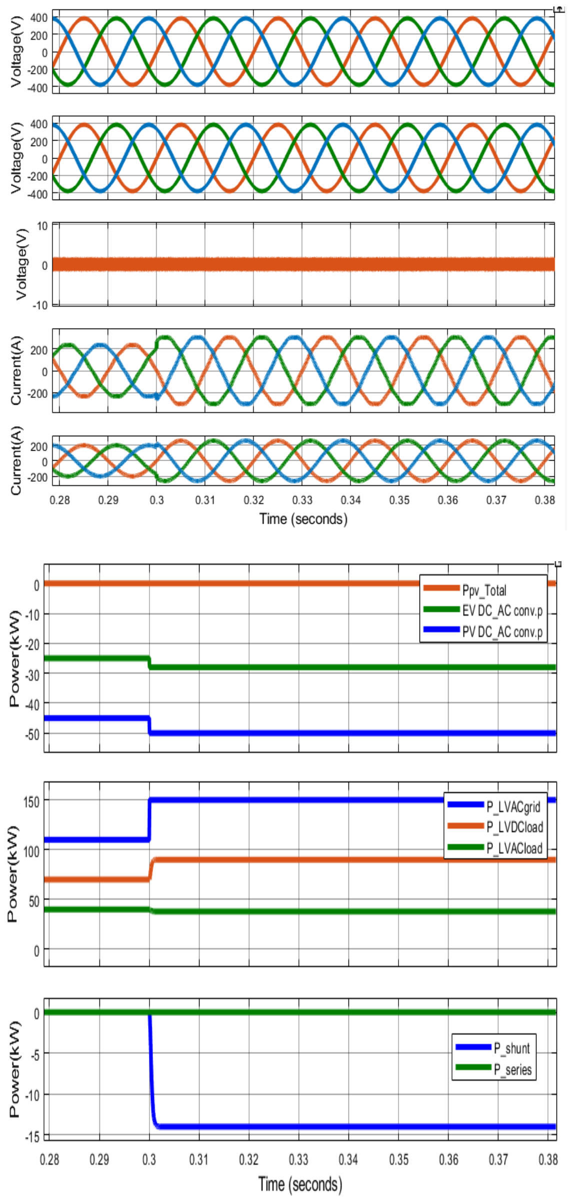

Figure 13: Results of the simulation for operating with a high DC load. (a) Voltage on the grid and (b) Voltage at the power conversion centre. The voltages of the UPQC series converters (c). d) Currents across the LV_{ac} load at the PCC. e. Currents in the grid. (f) The powers of photovoltaic (PV) generating, electric vehicles (EVs), and PV dc—ac converters. g) Powers generated by the Grid, LV_{ac} and LVdc. (h) Power from the UPQC shunt and the series converter.

The above simulation results shows the high dc load operation, when the load is increased suddenly the the converter powers smoothly changed to new value. Shows in the above simulation after 0.35.

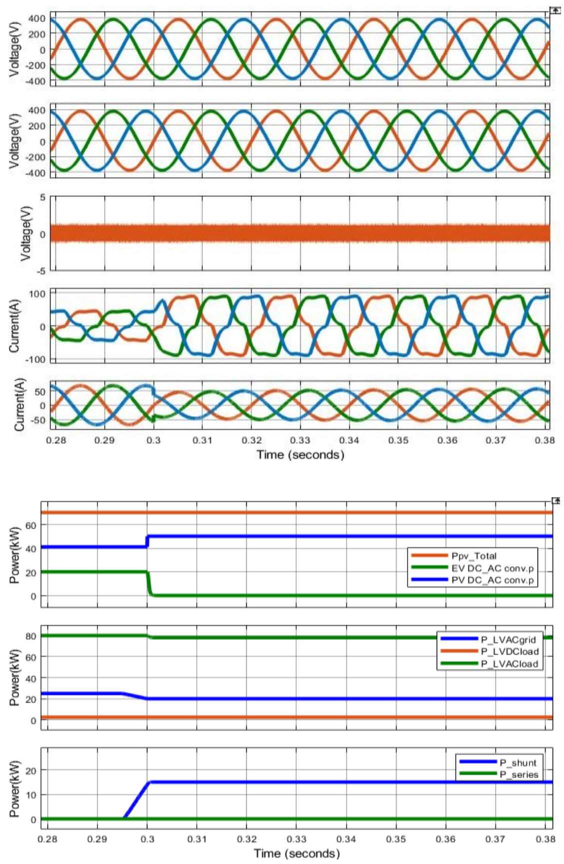

Fig.14 Results of the EV dc-ac converter failure operation simulation. (a) Voltages on the grid. (b) Voltages measured at the PCC. (c)The voltage of the UPQC series converter (d). Currents across the LV_{ac} load at the PCC. (e). Currents in the grid. (f) The powers of photovoltaic (PV) generating, electric vehicles (EVs), and PV dc—ac converters. g) Powers generated by the Grid, LV_{ac}, and LV_{dc}. (g) The UPQC shunt and series converter powers.

The above figure shows the converter failure operation while using FOSMC controller, after converter failure the converter power and PV and EV powers changes new value with smooth change and performance of the system is not disturbed.

COMPARISION TABLE

Parameter	**(PI Controller)**	**(FOSMC Controller)**	**Improvement**
Load Voltage THD (%)	1.74%	0.73%	↓ ~70–80%

Load Current THD (%)	2.64%	2.11%	↓ ~65–75%
Voltage Sag Compensation (%)	90 %	98%	Nearly ideal
Settling Time (ms)	60 ms	20 ms	Faster (~3×)
Rise Time (ms)	30 ms	10 ms	Faster
Steady-State Error	2 %	< 1 %	Highly accurate
Dynamic Response (Disturbances)	Moderate	Very Fast & Robust	Improved
DC-Link Voltage Regulation	Fluctuations present	Stable & smooth	Strong improvement
Power Factor	0.96	0.99	Near unity
Grid Current Quality	Distorted	Nearly sinusoidal	Improved
Converter Power Sharing	Less optimal	Efficient & balanced	Optimized
Robustness to Parameter Variations	Low	High	Strong improvement
Performance under EV Converter Failure	Partial compensation	Full compensation	Reliable
High DC Load Handling	Voltage deviations	Stable operation	Improved

CONCLUSION

Mesh hybrid AC/DC microgrids based on Fractional-Order Sliding Mode Controllers (FOSMCs) were the focus of this work. The proposed configuration enhances the voltage profile at the LVAC load buses and ensures higher power quality, allowing conventional distribution networks to host loads and produce more power. Faster dynamic response, increased resilience against parameter changes, and efficient disturbance rejection are all benefits of integrating FOSMC into the UPQC's series and shunt converters as opposed to standard PI-based control approaches. The suggested system ensures stable operation during failures of PV and EV DC-AC converters by distributing power across numerous converters and allows flexible power sharing LVAC and LVDC networks. Even in the face of uncertain renewable generation and dynamic demand, the DC-link may be stabilised and bidirectional power flow made feasible with the help of battery energy storage. The UPQC, which is managed by FOSMC, ensures that the voltage and current remain sinusoidally balanced at the point of common connection by reducing voltage dips, spikes, harmonics, and load imbalance. The suggested FOSMC-based UPQC beats traditional control approaches in three critical areas: dependability, stability of the system, and power quality improvement, as shown in simulation results under different operating situations. With its high penetration of renewable energy sources and electric car loads, a proposed meshed hybrid microgrid with FOSMC-controlled UPQC offers a reliable and cost-effective alternative to current distribution systems.

REFERENCES

[1] X. Liang, “Emerging power quality challenges due to integration of renewable energy sources,” *IEEE Trans. Ind. Appl.*, vol. 53, no. 2, pp. 855–866, Mar./Apr. 2017.

[2] R. Gupta, S. Doolla, and A. Chatterjee, “Hybrid AC–DC microgrid: Systematic evaluation of control strategies,” *IEEE Trans. Smart Grid*, vol. 9, no. 4, pp. 3830–3843, Jul. 2018.

[3] A. Alshahrani, M. Khalid, and M. Almuhaini, “Electric vehicles beyond energy storage and modern power networks: Challenges and applications,” *IEEE Access*, vol. 7, pp. 99031–99064, 2019.

[4] N. Thang, A. Ahmed, D. Kim, and J. Park, “Flexible system architecture of stand-alone PV

power generation with energy storage device," *IEEE Trans. Energy Convers.*, vol. 30, no. 4, pp. 1386–1396, Dec. 2015.

[5] J. von Appen, T. Braun, T. Stetz, K. Diwold, and D. Geibel, "Time in the sun: The challenge of high PV penetration in the German electric grid," *IEEE Power Energy Mag.*, vol. 11, no. 2, pp. 55–64, Mar./Apr. 2013.

[6] S. Chaudhary, J. M. Guerrero, and R. Teodorescu, "Enhancing the capacity of the AC distribution system using DC interlinks—A step toward future DC grid," *IEEE Trans. Smart Grid*, vol. 6, no. 4, pp. 1722–1729, Jul. 2015.

[7] Y. Liu, Y. Li, J. Zhang, Y. Feng, and J. Du, "V2G integration based on a UPQC with SMES," *IEEE Trans. Appl. Super cond.*, vol. 34, no. 8, pp. 1–3, Nov. 2024.

[8] C. Brandão, R. Santos, D. Silva, R. Oliveira, and O. Donoso-Garcia, "Model-free energy management system for hybrid AC/DC microgrids," *IEEE Trans. Ind. Electron.*, vol. 68, no. 5, pp. 3982–3991, May 2021.

[9] R. Zhu, M. Liserre, M. Langwasser, and P. Kumar, "Operation and control of the smart transformer in meshed and hybrid grids," *IEEE Ind. Electron. Mag.*, vol. 15, no. 1, pp. 43–57, Mar. 2021.

[10] J. Núñez, D. Posada, F. Unsihuay-Vila, and D. Pinzón-Ardila, "Review of smart transformer-based meshed hybrid microgrids," *IEEE Access*, vol. 11, pp. 130165–130185, 2023.

[11] H. Akagi, "New trends in active filters for power conditioning," *IEEE Trans. Ind. Appl.*, vol. 32, no. 6, pp. 1312–1322, Nov./Dec. 1996.

[12] M. Aredes, K. Heumann, and E. Watanabe, "An universal active power line conditioner," *IEEE Trans. Power Del.*, vol. 13, no. 2, pp. 545–551, Apr. 1998.

[13] B. Singh, A. Chandra, and K. Al-Haddad, *Power Quality: Problems and Mitigation Techniques*. Hoboken, NJ, USA: Wiley, 2015.

[14] V. Khadkikar, "Enhancing electric power quality using UPQC: A comprehensive overview," *IEEE Trans. Power Electron.*, vol. 27, no. 5, pp. 2284–2297, May 2012.

[15] M. Karimi-Ghartemani, "Enhanced phase-locked loop structures for power and energy applications," *IEEE Trans. Ind. Electron.*, vol. 61, no. 3, pp. 1464–1474, Mar. 2014.

[16] S. Kouro et al., "Recent advances and industrial applications of multilevel converters," *IEEE Trans. Ind. Electron.*, vol. 57, no. 8, pp. 2553–2580, Aug. 2010.

[17] J. M. Guerrero, P. C. Loh, T.-L. Lee, and M. Chandorkar, "Advanced control architectures for intelligent microgrids—Part I," *IEEE Trans. Ind. Electron.*, vol. 60, no. 4, pp. 1254–1262, Apr. 2013.

[18] Y. Levron, J. M. Guerrero, and Y. Beck, "Optimal power flow in microgrids with energy storage," *IEEE Trans. Power Syst.*, vol. 28, no. 3, pp. 3226–3234, Aug. 2013.

[19] I. Podlubny, *Fractional Differential Equations*. San Diego, CA, USA: Academic Press, 1999.

[20] S. Das, *Functional Fractional Calculus*. Berlin, Germany: Springer, 2011.

[21] Y. Shtessel, C. Edwards, L. Fridman, and A. Levant, *Sliding Mode Control and Observation*. New York, NY, USA: Springer, 2014.

[22] J. Liu and X. Wang, *Advanced Sliding Mode Control for Mechanical Systems*. Beijing, China: Tsinghua Univ. Press, 2012.

[23] H. Komurcugil, "Sliding-mode control strategy for single-phase grid-connected converters," *IEEE Trans. Ind. Electron.*, vol. 63, no. 10, pp. 6397–6408, Oct. 2016.

[24] A. Yazdani and R. Iravani, *Voltage-Sourced Converters in Power Systems*. Hoboken, NJ, USA: Wiley, 2010.

[25] M. Liserre, F. Blaabjerg, and S. Hansen, "Design and control of an LCL-filter-based grid-connected inverter," *IEEE Trans. Ind. Appl.*, vol. 41, no. 5, pp. 1281–1291, Sep./Oct. 2005.